sustainability

MDPI

Article

Applicability Evaluation of Energy Slabs Installed in an Underground Parking Lot

Seokjae Lee [1], Sangwoo Park [2], Taek Hee Han [1], Jongmuk Won [3] and Hangseok Choi [4,*]

[1] Coastal Development and Ocean Energy Research Center, Korea Institute of Ocean Science and Technology, Busan 49111, Republic of Korea
[2] Department of Civil Engineering and Environment Sciences, Korea Military Academy, Seoul 01805, Republic of Korea
[3] Department of Civil and Environmental Engineering, University of Ulsan, Ulsan 44610, Republic of Korea
[4] School of Civil, Environmental and Architectural Engineering, Korea University, Seoul 02841, Republic of Korea
* Correspondence: hchoi2@korea.ac.kr

Abstract: A floor slab of buildings can be used as a ground heat exchanger by equipping heat exchange pipes with a horizontal layout, namely energy slabs. The thermal performance of conventional energy slabs is relatively low due to the interference with the ambient air temperature. This fatal drawback can be overcome by installing energy slabs in an underground parking lot, where the influence of ambient air is not significant. This study experimentally investigated the applicability of two types of energy slabs (floor type and wall type), which were constructed on the basement slab in an underground parking lot. In particular, an aerogel-type thermal insulation layer was fabricated in each energy slab to isolate it from the ambient air along with enhancing the structural stability against automobiles. In the thermal performance tests, the constructed energy slabs showed a thermal performance 265% higher than the conventional energy slabs. Moreover, the aerogel-type thermal insulation layer effectively prevented surface condensation. However, the thermal stress of 2350 kPa was induced by the cooling operation in the energy slabs, which means the energy slab should possess sufficient tensile strength to secure the structural integrity of the parking lot basement.

Keywords: energy slab; ground heat exchanger; thermal insulation; thermal performance test; underground parking lot

Citation: Lee, S.; Park, S.; Han, T.H.; Won, J.; Choi, H. Applicability Evaluation of Energy Slabs Installed in an Underground Parking Lot. *Sustainability* **2023**, *15*, 2973. https://doi.org/10.3390/su15042973

Academic Editor: Firoz Alam

Received: 4 January 2023
Revised: 25 January 2023
Accepted: 3 February 2023
Published: 7 February 2023

1. Introduction

In order to cope with serious global climate change, various international efforts, such as the Kyoto Protocol (1997), RE100 (2014), and Paris Agreement (2015), are underway. In accordance with these worldwide trends, the government policies of many countries for encouraging the use of non-fossil energy sources made a rapid increase in the consumption of renewable energy (i.e., 2.6% per year), which exhibits the highest growth among other energy resources (i.e., nuclear power, natural gas, coal, etc.) [1]. Among the various types of renewable energy, the use of shallow geothermal energy offers an attractive option for heating and cooling buildings, which is known as a ground source heat pump (GSHP) system, due to its higher energy efficiency compared to conventional systems [2–4]. From 1995 to 2015, the worldwide installed capacity of GSHPs had increased from 1.8 GW to 50 GW [5]. The GSHP system consists of two main components, i.e., the heat pump and ground heat exchanger (GHEX). In general, a closed-loop vertical GHEX has been widely adopted in the GSHP system. This type of GHEX is installed by equipping plastic pipes in a vertically drilled borehole backfilled with grout material to induce a heat exchange between the circulating fluid and surrounding medium. However, the construction cost of the closed-loop vertical GHEX is significantly high, accounting for approximately 50% of the total installation cost of the GSHP system [6]. The high construction cost mainly

owing to additional borehole drilling may result in a prolonged payback period of the initial investment cost of the GSHP system. In order to reduce the total installation cost of the GSHP system, a closed-loop GHEX can be installed horizontally without a drilling process, which is called a closed-loop horizontal GHEX. However, the thermal performance of closed-loop horizontal GHEXs is too low to be adopted in the GSHP system because it is largely influenced by the ambient air temperature [7,8]. In addition, the closed-loop horizontal GHEXs are hard to be installed in a dense construction site because a considerable installation area is required when a long-length heat exchange pipe is installed to obtain a demanded thermal load [9].

Recently, several trials have been made to adopt the closed-loop horizontal GHEXs inside infra-structures to overcome the disadvantages. The energy wall secures the heat exchange performance by arranging heat exchange pipes (usually high-density polyethylene, HDPE) inside diaphragm walls [10,11]. Therefore, the energy wall can be adopted as a GHEX in the GSHP system after a temporal use of the diaphragm wall to support excavation surfaces and cutoff groundwater ingress while constructing underground structures. Sterpi et al. (2020) conducted a numerical study to propose an optimal heat exchange pipe layout in a diaphragm wall. According to their study, the diaphragm wall with a W-shape layout of heat exchange pipes enhanced the thermal performance by 10% comparing with a U-shape layout of heat exchange pipes [12]. Further, Barla et al. (2020) conducted a series of numerical studies to investigate the mechanical behavior induced by the heat exchange in the diaphragm wall [13]. The energy textile also assembles the closed-loop horizontal GHEX inside a tunnel lining to induce a heat exchange with ground formations [14]. Lee et al. (2016) conducted experimental and numerical studies to establish an artificial design for energy textiles [15]. Barla et al. (2019) installed a full-scale prototype energy tunnel (i.e., energy textile) in the Turin Metro Line 1, and thus investigated the thermal performance and thermal stress of the energy tunnel [16]. In addition, a numerical model was developed by calibrating the experimental results in the energy tunnel of Turin Metro Line 1, to provide an effective design tool [17]. Furthermore, Ma et al. (2022) developed a numerical model, which can simulate the thermo-hydro-mechanical behavior of the energy tunnel, for the safe design and sustainable long-term operation of the energy tunnel [18].

An energy slab is one of the hybrid structures that allows for utilizing geothermal energy by encasing the closed-loop horizontal GHEX in building slabs [19,20]. The energy slab can possess a long length of heat exchange pipes without the necessity of an additional construction site. However, its low thermal performance owing to direct exposure to ambient air is still an important issue to be addressed [21]. Therefore, Moon and Choi (2015) remarked that the energy slab should be combined with other types of GHEX, such as energy piles [22]. Meanwhile, equipping a thermal insulation layer inside the energy slab was introduced to relieve the effect of the ambient air temperature [23]. A Phenol foam (PF) board was proposed as an optimal material for thermal insulation in the energy slab, considering the insulation performance and economic feasibility [24]. This study introduced a novel way to improve the thermal performance of energy slabs by installing them in an underground parking lot, in which both the wall and floor slabs were utilized to install the energy slabs, and enabled producing more geothermal energy in the limited construction site. Further, the effect of the ambient air temperature on the energy slab was relieved compared to the previous study [23], which leads to a dramatic improvement in the thermal performance. Here, it is still necessary to assemble a thermal insulation layer inside the energy slabs to minimize the thermal interference induced by the ambient air in the underground parking lot. However, because the PF board is a closed-cell structure by foaming and curing the phenolic resin, it is vulnerable to external loads. That is, the PF board-type thermal insulation is inappropriate for the floor-type energy slabs on the basement floor in the underground parking lot, which can be stressed by automobile loads. In order to compensate for this unfavorable situation, aerogel-type thermal insulation was considered in this study. This new thermal insulation shows similar thermal conductivity to the PF board-type thermal insulation while having a thin and

flexible configuration. Therefore, the aerogel-type thermal insulation layer can be less vulnerable to automobile loads while securing enough of a thermal insulation performance. Meanwhile, surface condensation in the underground parking lot occurs generally due to the temperature difference between the ambient air and the surface of concrete slabs in the summer season. However, when energy slabs are installed in the underground parking lot, surface condensation should occur in the winter season because the heating operation of the GSHP system gradually decreases the temperature of the concrete slab lower than that of the ambient air. According to the previous study, the temperature in concrete slabs was approximately 10°C lower than ambient air, which can sufficiently cause surface condensation according to the humidity of the ambient air [23]. As automobiles constantly use the underground parking lot, surface condensation results in significant safety problems. Consequently, the applicability of the novel type of energy slab installed in underground parking lots should cover the assessment of both the thermal performance and surface condensation for future practice.

Periodic temperature changes in the heat exchange pipes can have a fatal effect on the integrity of infra-structures. The thermo-mechanical behavior induced by temperature changes in GHEXs has been extensively studied. For example, Adinolfi et al. (2021) conducted experimental and numerical studies on the thermo-mechanical behavior of the energy sheet pile wall [25]. Sterpi et al. (2017) analyzed the energy wall by the finite element analyses [26]. However, the stability of the energy slab corresponding to periodic temperature changes was not investigated yet.

This study experimentally investigates the applicability of two types of the energy slabs (floor type and wall type) equipped with the aerogel-type thermal insulation layer, which were constructed on the basement floor in an underground parking lot. The thermal performance tests (TPTs) were carried out in the constructed energy slabs, by simulating the cooling operation of the GSHP system. During the tests, the thermal performance of the energy slabs was investigated by measuring the inlet and outlet temperatures of the heat exchanger. In addition, the occurrence of surface condensation was determined by monitoring temperatures at the concrete slabs and comparing them with the ambient air temperature. Finally, the structural integrity of the energy slabs in the cooling operation was assessed from the measured temperatures and thermal stresses at the wall-type energy slab.

2. Construction of Energy Slabs in Underground Parking Lot

2.1. Overview of Construction Site

A residential building where the energy slabs were constructed is located in Daejeon city, Korea (Figure 1). This building consisted of two floors above the ground and one basement floor. The basement floor was constructed to make an underground parking lot and a machine room. Details of the residential building are summarized in Table 1. Before the construction, a subsurface geotechnical investigation was performed in the middle of the construction site, and the results are summarized in Table 2. The geological distributions were in the order of the buried layer, sedimentary layer, weathered soil layer, and weathered rock layer from the ground level. Further, the thermal conductivity of shallow ground formations (i.e., buried layer in this study) was measured by KD2-pro, which is based on the transient hot-probe method [23], because the energy slabs exchange heat energy mainly with the shallow ground formations. As shown in Figure 2, the thermal conductivity was estimated by averaging the measured values at three randomly selected locations in the ground where the basement floor was planned to be constructed. As a result, the average thermal conductivity of the buried layer was estimated to be 1.2 W/(m·K).

Figure 1. Overview of the residential building equipped with energy slabs.

Table 1. Details of the residential building equipped with energy slabs.

Type	Details
Location	Daejeon City, Korea
Purpose/Structure	Detached house/reinforced concrete
Land/Construction area	410 m^2/193 m^2
Total floor area	386 m^2
Building scale	One basement floor (parking lot and machine room), two ground floors
Height	9 m

Table 2. Results of subsurface geotechnical investigation.

Depth (m)	Division	Type	N-Value (Count/cm)
0.0~2.7	Buried layer	Silty sand with gravel	4/30~13/30
2.7~3.7	Sedimentary layer	Silty sand	5/30
3.7~11.0	Weathered soil	Silty sand	17/30~50/13
11.0~15.3	Weathered rock	Silty sand	50/7~50/10

Figure 2. Measurement locations of thermal conductivity on going-to-build basement floor. The Numbers (i.e., ①, ②, and ③) mean the thermal conductivity measurement locations.

2.2. Design of Energy Slab in Underground Parking Lot

Figure 3 shows the layouts of the constructed floor-type and wall-type energy slabs. The floor-type energy slab was constructed in the middle of the underground parking lot, while the wall-type energy slab was constructed on the wall of section A (refer to Figure 3a). Heat exchange pipes inside the energy slabs were assembled in a spiral configuration by maintaining the distance between adjacent heat exchange pipes (i.e., pitch) to be 400 mm. Note that the heat exchange pipes in the outlet parts (i.e., sections B and C in Figure 3a,b, respectively) were thermally insulated to control the pitch of 400 mm in the energy slabs. The specifications of the constructed energy slabs are summarized in Table 3.

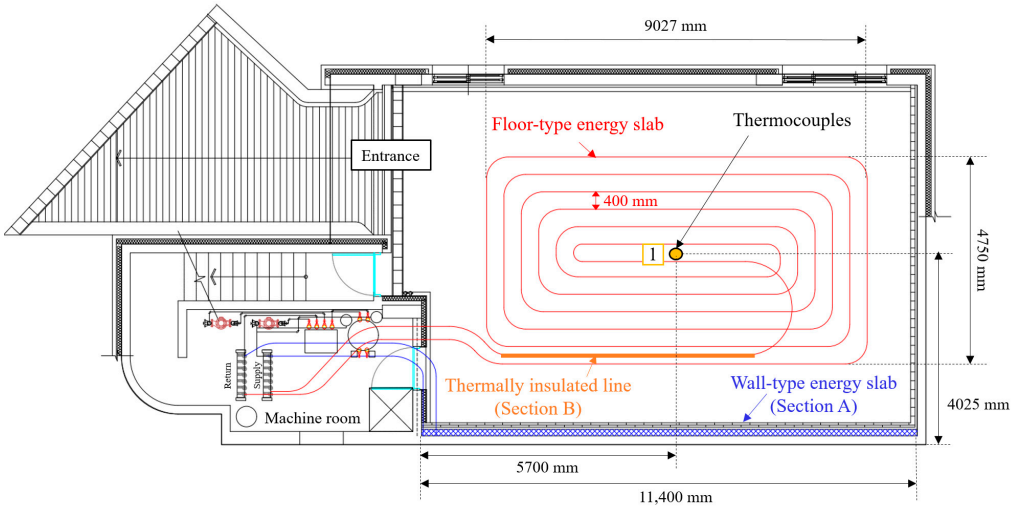

(**a**) Energy slabs in the underground parking lot

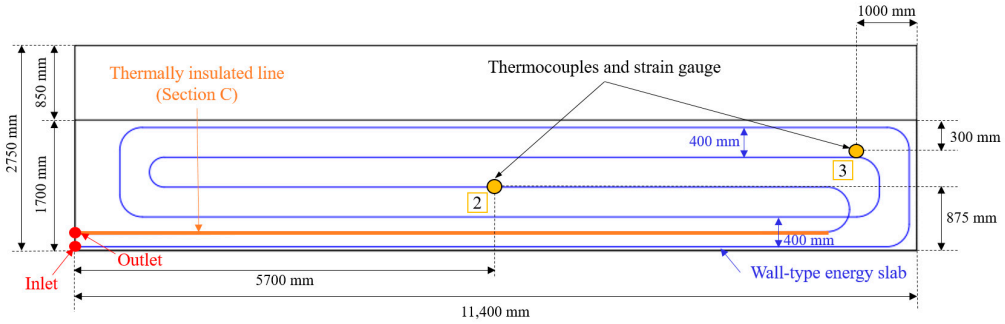

(**b**) Details of section A (wall-type energy slab)

Figure 3. Floor plans of constructed floor-type and wall-type energy slabs.

Table 3. Specifications of constructed energy slabs.

Type of Energy Slab	Pipe Material	Pipe Diameter (mm)	Pitch (mm)	Installation Area (m^2)	Total Length (m)
Floor type	High-density polyethylene (HDPE)	25	400	49.5	123
Wall type				18.5	55

As previously described, thermal insulation should be equipped in the energy slab to secure stable thermal performance. Moreover, surface condensation is expected to occur on the surface of slab concrete during the winter season owing to temperature variations in the heat exchange pipes (Figure 4a). This leads to a severe safety problem on the basement floor in the underground parking lot. In order to prevent surface condensation, the lower concrete slab possessing the heat exchange pipes should be thermally insulated from the upper concrete slab that directly contacts ambient air, as shown in Figure 4. As previously

mentioned, the PF board-type thermal insulation is inappropriate for the floor-type energy slabs in the underground parking lot, because the slabs can be stressed by automobile loads. In this study, aerogel-type thermal insulation was devised for the constructed energy slabs. This thermal insulation consisted of Pyrogel XT-E, whose thermal conductivity is 0.02 W/(m·K) at 38 °C according to the manufacturer's product declaration. In other words, the aerogel-type thermal insulation had similar thermal conductivity to the PF board-type thermal insulation (i.e., 0.018 W/(m·K)). In particular, the aerogel-type thermal insulation is more suitable for the energy slab in the underground parking lot due to its flexible and thin configuration. The sectional views of the constructed energy slabs are illustrated in Figure 5.

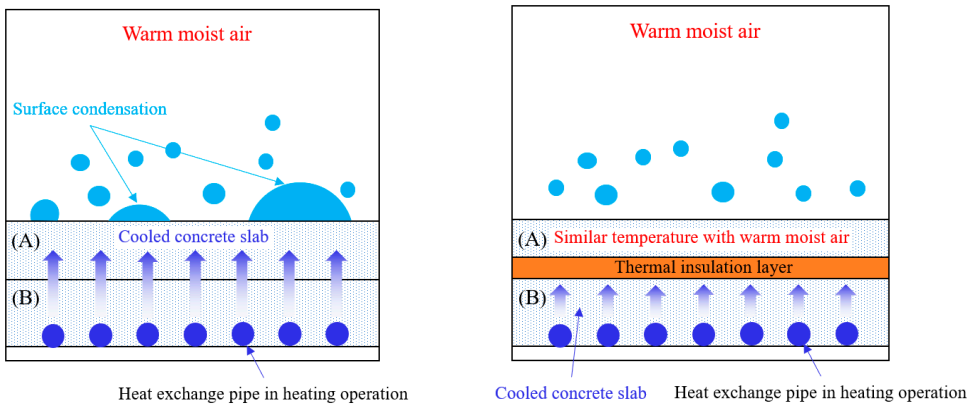

(**a**) Without thermal insulation (**b**) With thermal insulation

Figure 4. Schematic diagram when energy slab with and without thermal insulation layer during heating operation: (A) concrete slab contact with ambient air; (B) concrete slab possessing heat exchange pipes.

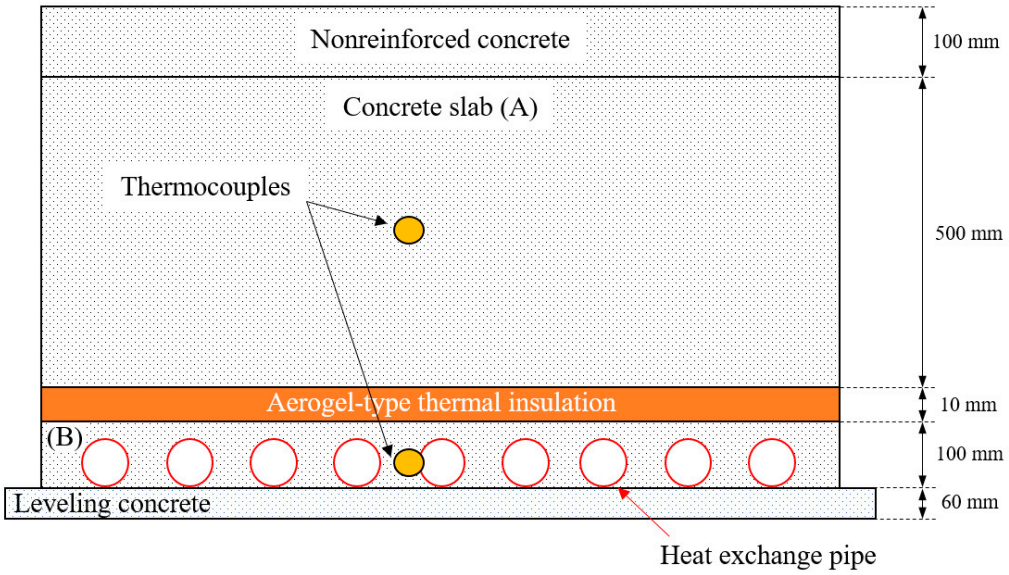

(**a**) Floor-type energy slab

Figure 5. *Cont.*

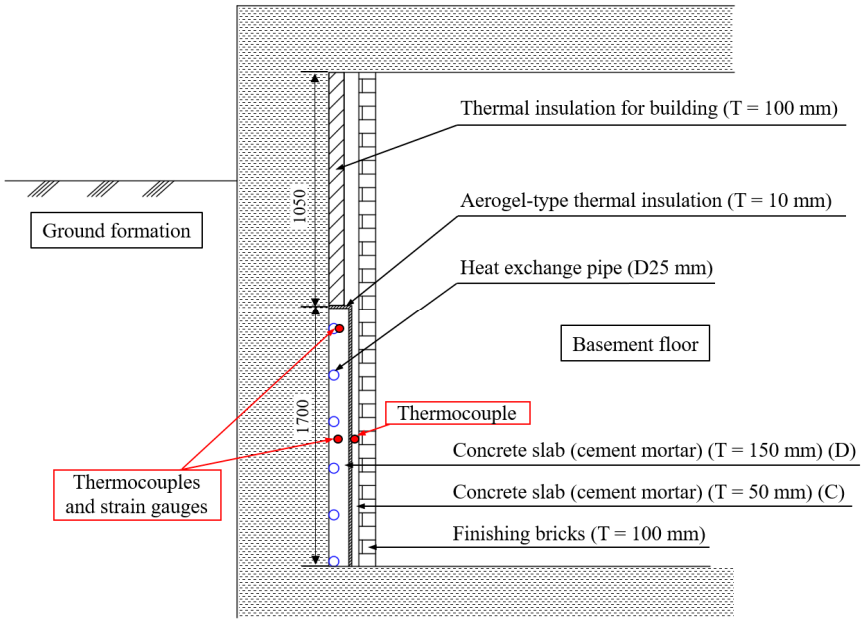

(**b**) Wall-type energy slab

Figure 5. Sectional views of constructed energy slab: (A) and (C) concrete slabs above aerogel-type thermal insulation layer, (B) and (D) concrete slabs possessing heat exchange pipes.

T-type thermocouples were equipped in the concrete slabs above the aerogel-type thermal insulation layer and the lower concrete slabs containing the heat exchange pipes, as shown in Figure 5, to examine surface condensation during the tests. Meanwhile, strain gauges (PMFL-60-2LT) were equipped inside the wall-type energy slab to investigate the thermo-mechanical behavior of the wall-type energy slab corresponding to temperature changes (Figure 5b). The installation locations of the T-type thermocouples and the strain gauges are summarized in Table 4.

Table 4. Detailed locations of thermocouples and strain gauges.

Type of Energy Slab	Locations		Sensor Type	Name
	Floor Plan	Slab Type		
Floor-type energy slab	1 (Figure 3a)	Concrete slab above aerogel-type thermal insulation ((A) in Figure 5a)	T-type thermocouple	T1A
		Concrete slab possessing heat exchange pipe ((B) in Figure 5a)	T-type thermocouple	T1B
Wall-type energy slab	2 (Figure 3b)	Concrete slab above aerogel-type thermal insulation ((C) in Figure 5b)	T-type thermocouple	T2C
		Concrete slab possessing heat exchange pipe ((D) in Figure 5b)	T-type thermocouple Strain gauge	T2D S2D
	3 (Figure 3b)	Concrete slab possessing heat exchange pipe ((D) in Figure 5b)	T-type thermocouple Strain gauge	T3D S3D

2.3. Construction Procedure of Energy Slabs

Figures 6 and 7 show construction procedures of the floor-type and wall-type energy slabs, respectively. Both energy slabs were constructed under a similar procedure: arranging

and fixing heat exchange pipes, connecting the return and supply pipes, pouring concrete on each slab, and installing aerogel-type thermal insulation. Particularly, in case of the floor-type energy slab, the construction was finished after the 2nd concrete pouring and concrete leveling. On the other hand, the wall-type energy slab was finally made by pouring cement mortar and installing finishing bricks.

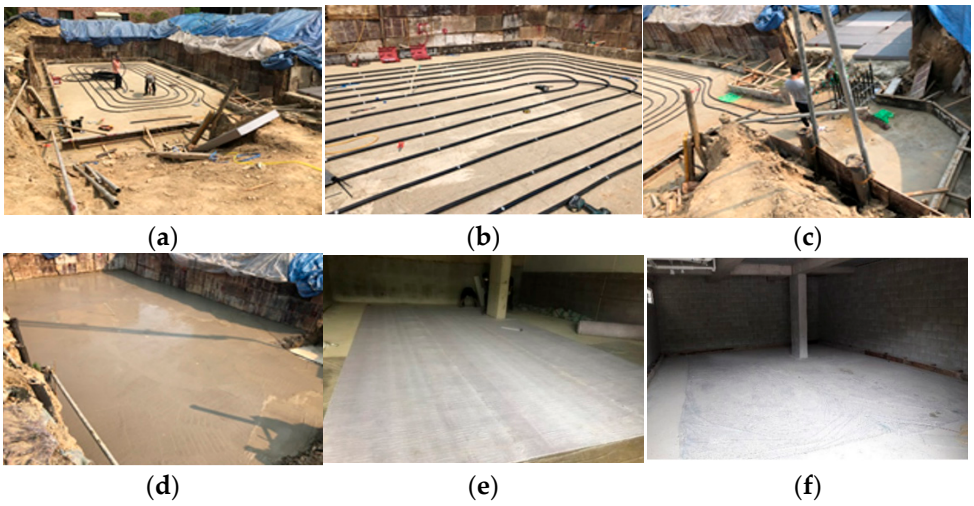

Figure 6. Construction procedure of floor-type energy slab. (**a**) Arrangement of heat exchange pipes. (**b**) Fixing heat exchange pipes. (**c**) Connection of supply and return pipe. (**d**) Placement of concrete on floor slab. (**e**) Installation of aerogel-type thermal insulation. (**f**) Placement of concrete to adjust leveling.

Figure 7. Construction procedure of wall-type energy slab. (**a**) Arrangement of heat exchange pipes. (**b**) Fixing heat exchange pipes. (**c**) Connection of supply and return pipe. (**d**) Placement of concrete on wall slab. (**e**) Installation of aerogel-type thermal insulation. (**f**) Placement of cement mortar and installation of bricks.

3. In Situ Thermal Performance Test (TPTs) with Constructed Energy Slabs

3.1. Experimental Conditions for In Situ TPT

In order to evaluate the thermal performance, surface condensation, and structural stability of the constructed energy slabs, a series of in situ TPTs was conducted in the test bed. The in situ TPT was proposed to evaluate the thermal performance of GHEXs by simulating artificial heating or cooling loads [23,27]. In this study, artificial thermal loads were supplied to the constructed energy slabs by maintaining the inlet temperature and the flow rate of a working fluid with the aid of a constant-temperature water bath (refer

to Table 5 [23] and Figure 8). During the tests, changes in the outlet temperature were continuously measured. Then, the thermal performances of the constructed energy slabs were evaluated by calculating heat exchange amounts through Equation (1) [23].

$$Q = C \times \dot{m} \times |T_{out} - T_{in}| \quad (1)$$

where Q is the heat exchange amount (W), C is the specific heat capacity of the working fluid (J/(kg·K)), $\dot{m}$ is the mass flux of circulating fluid (kg/s), and T_{in} and T_{out} are the inlet and outlet temperatures, respectively (°C).

Table 5. Specifications of constant-temperature water bath [23].

Type	Details
Bath size (dimension, W × D × H mm)	350 × 400 × 300 mm
Bath capacity	42 L
Power of heater/cooler	4.0 kW/0.6 kW
Range of temperature capacity	−10 °C~98 °C
Temperature uniformity	±1 °C
Capacity of circulation pump	20 L/min
Electric requirement	220 VAC, 60 Hz

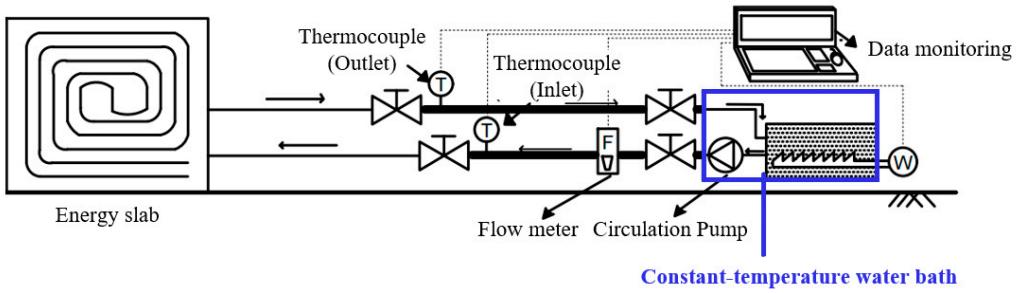

Figure 8. Schematic diagram of thermal performance test (TPT).

Figure 9 shows the experimental setup and monitoring instruments established in the machine room (refer to Figure 3a). The inlet temperature was kept constant at 25 °C during the TPTs to simulate cooling operation and continuously monitored by the T-type thermocouple, as depicted in Figure 8. The flow rate of a working fluid was determined to be 7.4 L/min to satisfy the Reynolds number greater than 4000, which is the threshold value to generate fully turbulent flow inside the pipes [23]. An intermittent operation of 8 h operation and 16 h pause was applied to replicate the heat pump operation in commercial buildings. The TPTs were conducted for seven continuous days. During the TPTs, the temperatures of outlet fluid, which finished heat exchange with the ground formations, were measured using the T-type thermocouple, as illustrated in Figure 8. Finally, the average heat exchange amounts of the energy slabs were calculated by using the flow rate of working fluid and the measured inlet and outlet temperatures.

3.2. Result of TPTs

Figure 10 shows the measured inlet and outlet temperatures and the flow rate of the working fluid during the TPTs at each energy slab. The temperature differences (i.e., the heat exchange with the surrounding ground) occurred only during the operation phases when the flow rate of a working fluid was generated at 7.4 L/min. The average temperature difference during the TPTs was more than 2 °C, indicating a stable heat exchange was obtained in both types of the energy slabs. The average heat exchange amounts of the floor-type and the wall-type energy slabs were 2260 W and 866 W, respectively. Further, the average heat exchange amounts per unit area of the floor-type and the wall-type energy slabs were 45.7 W/m^2 and 46.8 W/m^2, respectively. Because both types of the energy slabs had the identical configuration for the heat exchange pipes (i.e., a spiral configuration

with 400 mm pitch), a similar average heat exchange amount per unit area was obtained. In other words, the thermal performance of the energy slab was more influenced by the configuration of the heat exchange pipes, not the structure type (i.e., wall type or floor type).

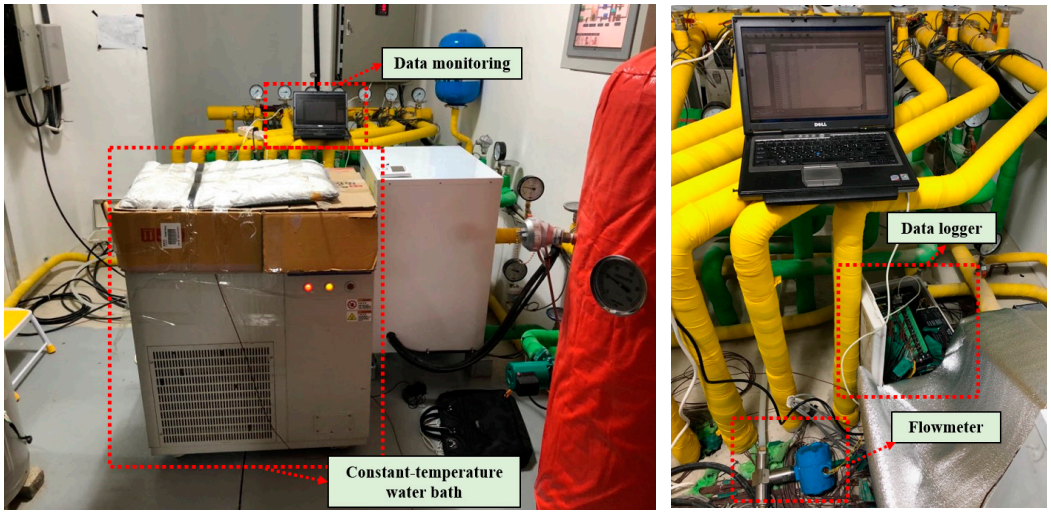

Figure 9. Overview of experimental setup and monitoring instruments established in machine room.

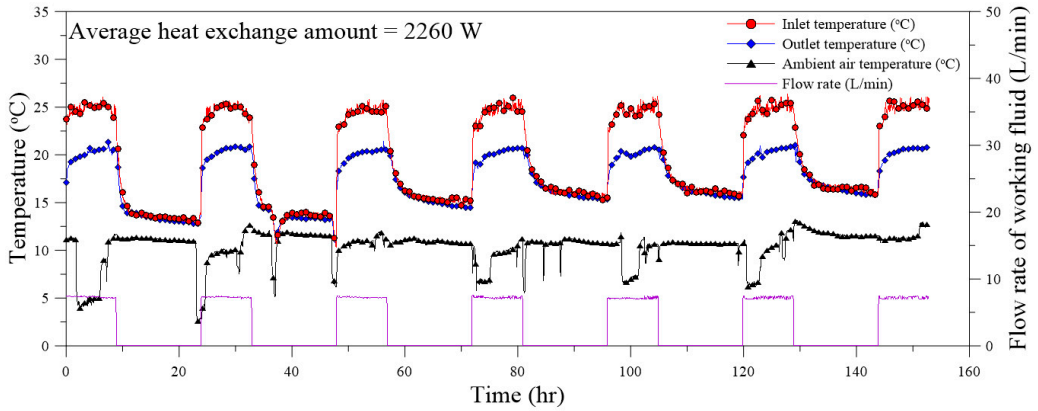

(**a**) Floor-type energy slab

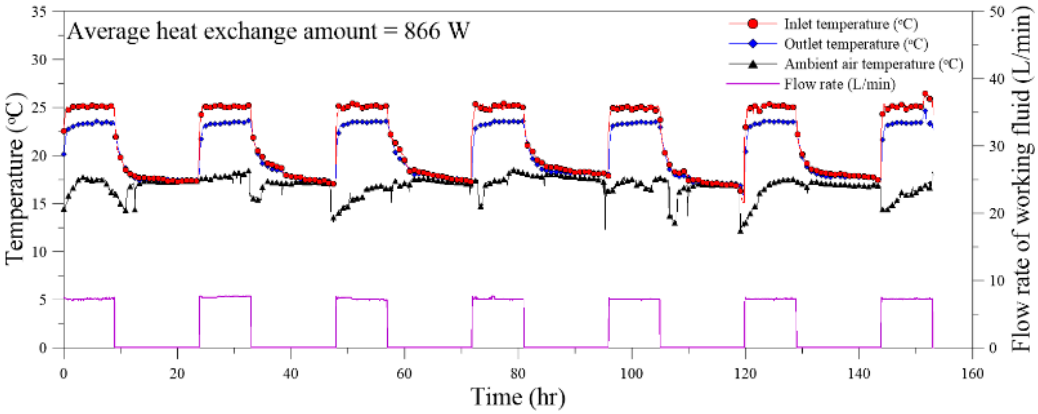

(**b**) Wall-type energy slab

Figure 10. Measured inlet, outlet, and ambient air temperatures and flow rate of working fluid during TPTs.

In order to investigate the applicability of the energy slabs in more detail, the thermal performance of the floor-type energy slab in this study was compared with that of the

floor-type energy slab discussed in the previous study [23]. Table 6 shows the construction conditions and the TPT results of the two floor-type energy slabs. Although the energy slab studied by Lee et al. (2018) exchanged the heat energy with the surrounding ground with 171% higher thermal conductivity and a 125% denser configuration of the heat exchange pipes than the energy slabs in this study, the present energy slabs showed the average heat exchange amount per unit area was 265% greater than Lee et al. (2018). This is attributable to the fact that the energy slab of Lee et al. (2018) was constructed on the ground surface, and thus the ambient air temperature could significantly interfere with the heat transfer in the energy slab, even when equipped with PF board-type thermal insulation (refer to Figure 11 [23]). On the other hand, the energy slab in this study effectively relieved the influence of the ambient air by installing below the ground surface (i.e., in the underground parking lot). Such a favorable construction condition significantly improved the thermal performance.

Table 6. Comparison on construction conditions and TPT results of floor-type energy slabs between the present study and Lee et al. (2018) [23].

Type	Floor-Type Energy Slab in This Study	Floor-Type Energy Slab in Previous Study [23]
Heat exchange pipe material (diameter)	HDPE (25 mm)	
Total length of heat exchange pipe	123 m	85 m
Pitch	400 mm	300 mm
Installation area	49.5 m^2	25 m^2
Density of heat exchange pipe (Total length of heat exchange pipe/ Installation area)	2.73 m/m^2	3.4 m/m^2
Thermal conductivity of ground formation	1.2 W/(m·K)	2.05 W/(m·K)
Thermal conductivity of thermal insulation material	0.02 W/(m·K) (Aerogel)	0.018 W/(m·K) (Phenol foam (PF) board)
Average heat exchange amount (7 days)	2260 W	430 W
Average heat exchange amount per unit area	45.7 W/m^2	17.2 W/m^2

3.3. Investigation of Surface Condensation

The occurrence of surface condensation in the energy slabs was examined by monitoring the temperature changes at the T-type thermocouples installed in each concrete slab (i.e., T1A, T1B, T2C, and T2D in Table 4) during the TPTs. Figure 12 shows the temperature variations corresponding to the locations of the thermocouples. The temperatures in the concrete slabs equipped with heat exchange pipes (i.e., below the aerogel-type thermal insulation, T1B and T2D) repeatedly increased and decreased in accordance with the intermittent operation of the constant-temperature water bath. Meanwhile, the temperatures in the concrete slabs located above the aerogel-type thermal insulation layer (i.e., T1A and T2C) were changed regardless of the intermittent operation. Rather, they showed a similar trend in the ambient air temperature. This result indicates that the concrete slab above the aerogel-type thermal insulation layer and the lower concrete slab possessing heat exchange pipes became thermally isolated by installing the aerogel-type thermal insulation. That is,

surface condensation may not occur on the constructed energy slabs in the underground parking lot even though the temperatures in the lower concrete slab become lower than that of the ambient air during the heating operation of the GSHP system.

Figure 11. Overview of energy slab constructed by Lee et al. (2018) [23].

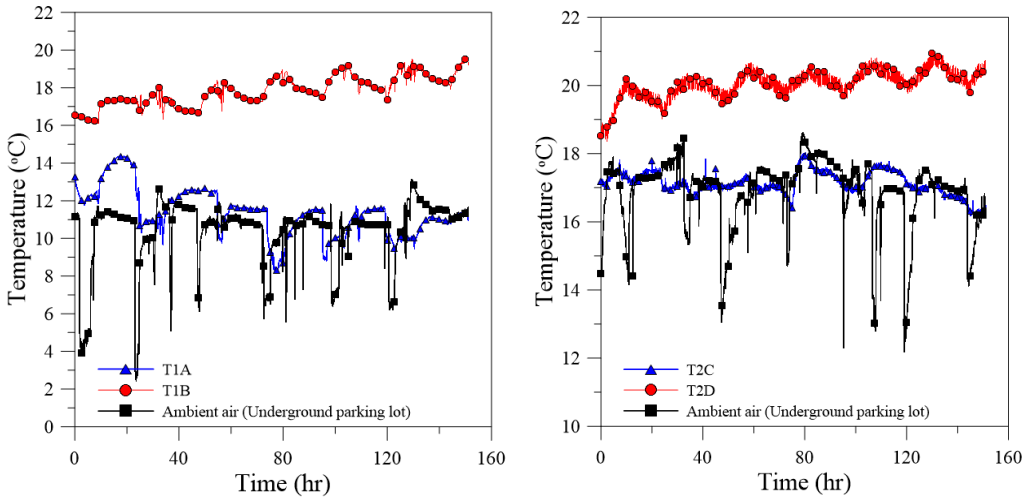

(**a**) Floor-type energy slab (**b**) Wall-type energy slab

Figure 12. Temperature variations in concrete slab above aerogel-type thermal insulation, lower concrete slab possessing heat exchange pipe, and ambient air during TPTs according to energy slab types.

4. Structural Stability of Energy Slab in Underground Parking Lot

During the heat pump operations in a GSHP system, a temperature reduction in the energy slab (i.e., heating operation) shrinks the concrete, and a temperature increase in the energy slab (i.e., cooling operation) expands the concrete, which may cause thermal stress on the energy slab. This can be a potential threat to the structural integrity of the energy slab. In this study, the thermal stress in the wall-type energy slab was investigated by simultaneously measuring the temperature changes in T2D, T3D, S2D, and S3D during the TPTs. Note that the strains in S2D and S3D were measured at the end of each operation phase.

Figure 13 shows the temperature changes and thermal stress at the concrete slab possessing the heat exchange pipes during the TPTs. The thermal stresses were calculated by the measured strains, assuming the elastic modulus of the slab cement to be 36,500 MPa, referring to the previous study [28].

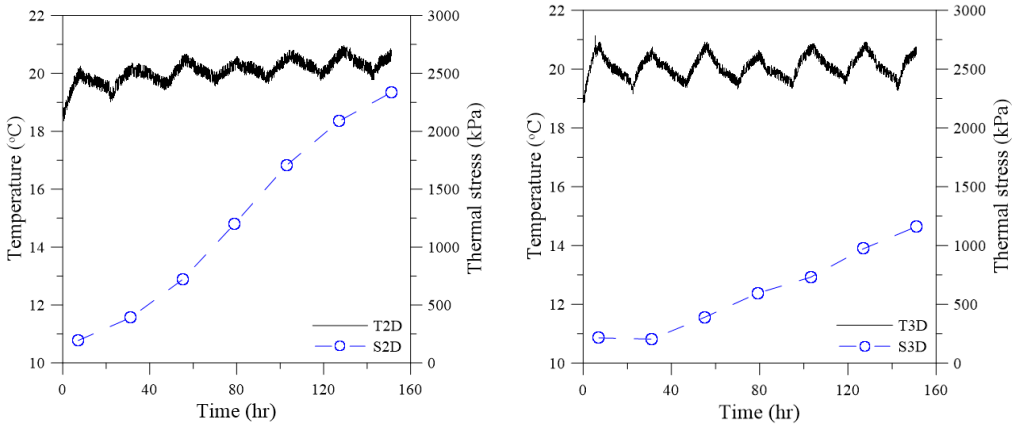

(**a**) Center of wall-type energy slab (**b**) Corner of wall-type energy slab

Figure 13. Temperature changes and thermal stress at concrete slab possessing heat exchange pipe during TPTs.

As illustrated in Figure 13, the thermal stresses were accumulated owing to the continuously elevated temperature in the concrete (i.e., T2D and T3D) from the initial stage. In addition, the thermal stress at the center of the concrete slab (i.e., S2D) was larger than that at the corner of the concrete slab (i.e., S3D). Because S3D was located at the corner of the wall-type energy slab, as shown in Figure 3b, the strain was restricted by the nearby building structures. On the other hand, because S2D was located at the center of the wall-type energy slab, as shown in Figure 3b, the strain restriction in S2D was less significant than that in S3D, which increased the thermal stresses as well. As a result, the thermal stress at the center of the wall-type energy slab was approximately 2350 kPa at the end of the TPT, which is higher than that at the corner of the wall-type energy slab by as much as 1100 kPa (Figure 13). In the previous study, the tensile and compressive strengths of the concrete were varied with the properties of the cement mortar [28–30]. In particular, the tensile strength of cement mortar is commonly smaller than 2 MPa [29,30]. That is, according to the result of this study, the structural integrity of the energy slabs can be threatened by excessive thermal stress. Consequently, it is necessary to secure enough tensile strength of the cement mortar for the energy slab, specially to manage the thermal stress induced by the cooling operation. Note that, in this paper, the structural stability of the energy slab installed in the underground parking lot was investigated only in the cooling operation of the thermal performance tests (TPTs). In addition, the tests were performed for seven days in accordance with the previous study, which conducted the TPT to evaluate the thermal performance of energy slabs [23]. Therefore, there are some limitations in this study to be addressed in future works. The thermal stress induced by not only the cooling operation but also the heating operation of the TPT should be investigated for the comprehensive evaluation on the structural stability of the constructed energy slab. Moreover, because the thermal stress is accumulated with the test progress (refer to Figure 13), a long-term TPT (i.e., more than seven days) should be performed to obtain the maximum thermal stress in the constructed energy slab.

5. Conclusions

The conventional energy slab is hard to be adopted in a practical GSHP system owing to its low thermal performance, even with the utilization of thermal insulation. Considering the increment of energy slab utilization, a novel type of the energy slab was devised in this study, which is installed in an underground parking lot equipped with aerogel-type thermal insulation. With this approach, the influence of the ambient air temperature is expected to be minimized, leading to a dramatic improvement in the thermal performance of the energy slab. In this study, the energy slabs equipped with aerogel-type thermal insulation were installed in the underground parking lot to investigate their thermal behaviors by

performing a series of TPTs. Then, the thermal performance, the occurrence of surface condensation, and the structural integrity were investigated by analyzing the TPT results. The followings are the primary findings of this study.

1. The floor- and wall-type energy slabs equipped with aerogel-type thermal insulation showed a stable thermal performance in the underground parking lot. In particular, the energy slabs in this study increased the average heat exchange amount per unit area by 265% in comparison with the previous study, by reducing the thermal interference induced by the ambient air temperature.
2. The aerogel-type thermal insulation layer thermally isolated the concrete slabs with the heat exchange pipes from the ambient air refrained from surface condensation. This is especially critical when the temperature in the concrete slab encasing the heat exchange pipes becomes lower than the ambient air temperature during the heating operation of the GSHP system.
3. The maximum thermal stress was estimated to be approximately 2350 kPa at the end of the TPT. Therefore, it is necessary to secure enough tensile strength of the cement mortar for the energy slab, specially to manage the thermal stress induced by the cooling operation.
4. The present study's limitations are that the structural stability of the energy slab installed in the underground parking lot was investigated only in the cooling operation of the thermal performance tests (TPTs), and the tests were performed for seven days in accordance with the previous study. In future works, to overcome such limitations, the TPT in the heating operation should be performed to comprehensively quantify the effect of thermal stress on the structural stability of the energy slab. Furthermore, the maximum thermal stress is also necessary to be checked by performing a long-term TPT.

Author Contributions: Conceptualization, H.C.; Methodology, S.L., S.P. and T.H.H.; Validation, S.P., T.H.H. and J.W.; Data curation, J.W.; Writing—original draft, S.L.; Writing—review & editing, H.C.; Funding acquisition, H.C. All authors have read and agreed to the published version of the manuscript.

Funding: This research was funded by National Research Foundation of Korea grant number 2020R1A6A1A03045059 and 2022R1C1C2003462.

Institutional Review Board Statement: Not applicable.

Informed Consent Statement: Not applicable.

Data Availability Statement: Some or all data, models, or code that support the findings of this study are available from the corresponding author upon reasonable request.

Conflicts of Interest: The authors declare no conflict of interest.

References

1. Conti, J.; Holtberg, P.; Diefenderfer, J.; LaRose, A.; Turnure, J.T.; Westfall, L. *International Energy Outlook 2016 with Projections to 2040*; USDOE Energy Information Administration (EIA): Washington, DC, USA, 2016.
2. Liu, R.; Salem, M.; Rungamornrat, J.; Al-Bahrani, M. A Comprehensive and Updated Review on the Exergy Analysis of Ground Source Heat Pumps. *Sustain. Energy Technol. Assess.* **2023**, *55*, 102906. [CrossRef]
3. Huang, B.; Mauerhofer, V. Life Cycle Sustainability Assessment of Ground Source Heat Pump in Shanghai, China. *J. Clean. Prod.* **2016**, *119*, 207–214. [CrossRef]
4. Hepbasli, A.; Akdemir, O. Energy and Exergy Analysis of a Ground Source (Geothermal) Heat Pump System. *Energy Convers. Manag.* **2004**, *45*, 737–753. [CrossRef]
5. Kumar, S.; Murugesan, K. Optimization of Geothermal Interaction of a Double U-Tube Borehole Heat Exchanger for Space Heating and Cooling Applications Using Taguchi Method and Utility Concept. *Geothermics* **2020**, *83*, 101723. [CrossRef]
6. Blum, P.; Campillo, G.; Kölbel, T. Techno-Economic and Spatial Analysis of Vertical Ground Source Heat Pump Systems in Germany. *Energy* **2011**, *36*, 3002–3011. [CrossRef]
7. Esen, H.; Inalli, M.; Esen, M.; Pihtili, K. Energy and Exergy Analysis of a Ground-Coupled Heat Pump System with Two Horizontal Ground Heat Exchangers. *Build. Environ.* **2007**, *42*, 3606–3615. [CrossRef]

8. Tarnawski, V.R.; Leong, W.H.; Momose, T.; Hamada, Y. Analysis of Ground Source Heat Pumps with Horizontal Ground Heat Exchangers for Northern Japan. *Renew. Energy* **2009**, *34*, 127–134. [CrossRef]
9. Dinh, B.H.; Kim, Y.-S.; Yoon, S. Experimental and Numerical Studies on the Performance of Horizontal U-Type and Spiral-Coil-Type Ground Heat Exchangers Considering Economic Aspects. *Renew. Energy* **2022**, *186*, 505–516. [CrossRef]
10. Xia, C.; Sun, M.; Zhang, G.; Xiao, S.; Zou, Y. Experimental Study on Geothermal Heat Exchangers Buried in Diaphragm Walls. *Energy Build.* **2012**, *52*, 50–55. [CrossRef]
11. Peterson, E.L.; Shafagh, I. Evaluation of Diaphragm Wall Heat Exchanger Potential. *Energy Build.* **2022**, *266*, 112107. [CrossRef]
12. Sterpi, D.; Tomaselli, G.; Angelotti, A. Energy Performance of Ground Heat Exchangers Embedded in Diaphragm Walls: Field Observations and Optimization by Numerical Modelling. *Renew. Energy* **2020**, *147*, 2748–2760. [CrossRef]
13. Barla, M.; di Donna, A.; Santi, A. Energy and Mechanical Aspects on the Thermal Activation of Diaphragm Walls for Heating and Cooling. *Renew. Energy* **2020**, *147*, 2654–2663. [CrossRef]
14. Bidarmaghz, A.; Narsilio, G.A. Heat Exchange Mechanisms in Energy Tunnel Systems. *Geomech. Energy Environ.* **2018**, *16*, 83–95. [CrossRef]
15. Lee, C.; Park, S.; Choi, H.-J.; Lee, I.-M.; Choi, H. Development of Energy Textile to Use Geothermal Energy in Tunnels. *Tunn. Undergr. Space Technol.* **2016**, *59*, 105–113. [CrossRef]
16. Barla, M.; di Donna, A.; Insana, A. A Novel Real-Scale Experimental Prototype of Energy Tunnel. *Tunn. Undergr. Space Technol.* **2019**, *87*, 1–14. [CrossRef]
17. Insana, A.; Barla, M. Experimental and Numerical Investigations on the Energy Performance of a Thermo-Active Tunnel. *Renew. Energy* **2020**, *152*, 781–792. [CrossRef]
18. Ma, C.; di Donna, A.; Dias, D. Numerical Study on the Thermo-Hydro-Mechanical Behaviour of an Energy Tunnel in a Coarse Soil. *Comput. Geotech.* **2022**, *151*, 105003. [CrossRef]
19. Kayaci, N.; Demir, H.; Kanbur, B.B.; Atayilmaz, Ş.O.; Agra, O.; Acet, R.C.; Gemici, Z. Experimental and Numerical Investigation of Ground Heat Exchangers in the Building Foundation. *Energy Convers. Manag.* **2019**, *188*, 162–176. [CrossRef]
20. Nam, Y.; Chae, H.-B. Numerical Simulation for the Optimum Design of Ground Source Heat Pump System Using Building Foundation as Horizontal Heat Exchanger. *Energy* **2014**, *73*, 933–942. [CrossRef]
21. Choi, J.-M.; Sohn, B.-H. Performance Analysis of Energy-Slab Ground-Coupled Heat Exchanger. *Korean J. Air-Cond. Refrig. Eng.* **2012**, *24*, 487–496.
22. Moon, C.-E.; Choi, J.M. Heating Performance Characteristics of the Ground Source Heat Pump System with Energy-Piles and Energy-Slabs. *Energy* **2015**, *81*, 27–32. [CrossRef]
23. Lee, S.; Park, S.; Kang, M.; Choi, H. Field Experiments to Evaluate Thermal Performance of Energy Slabs with Different Installation Conditions. *Appl. Sci.* **2018**, *8*, 2214. [CrossRef]
24. Lee, S.; Park, S.; Won, J.; Choi, H. Influential Factors on Thermal Performance of Energy Slabs Equipped with an Insulation Layer. *Renew. Energy* **2021**, *174*, 823–834. [CrossRef]
25. Adinolfi, M.; Loria, A.F.R.; Laloui, L.; Aversa, S. Experimental and Numerical Investigation of the Thermo-Mechanical Behaviour of an Energy Sheet Pile Wall. *Geomech. Energy Environ.* **2021**, *25*, 100208. [CrossRef]
26. Sterpi, D.; Coletto, A.; Mauri, L. Investigation on the Behaviour of a Thermo-Active Diaphragm Wall by Thermo-Mechanical Analyses. *Geomech. Energy Environ.* **2017**, *9*, 1–20. [CrossRef]
27. Miyara, A.; Tsubaki, K.; Inoue, S.; Yoshida, K. Experimental Study of Several Types of Ground Heat Exchanger Using a Steel Pile Foundation. *Renew. Energy* **2011**, *36*, 764–771.
28. Yurtdas, I.; Burlion, N.; Skoczylas, F. Experimental Characterisation of the Drying Effect on Uniaxial Mechanical Behaviour of Mortar. *Mater. Struct.* **2004**, *37*, 170–176. [CrossRef]
29. Chen, X.; Wu, S.; Zhou, J. Influence of Porosity on Compressive and Tensile Strength of Cement Mortar. *Constr. Build. Mater.* **2013**, *40*, 869–874. [CrossRef]
30. Singh, S.B.; Munjal, P.; Thammishetti, N. Role of Water/Cement Ratio on Strength Development of Cement Mortar. *J. Build. Eng.* **2015**, *4*, 94–100. [CrossRef]